Supplementary Materials

Materials and Methods

Evaluation of SLE pathology

MRL.Fas^{lpr} SLE cohorts were analyzed as previously described (1, 2). For skin disease, mice were scored based on the extent of lesions on the dorsum of the neck and back. Macroscopic surface area was scored from 0 to 5 for an affected area up to 9.1 cm^2, with up to 1 additional point for the presence of ear (1/4 point each) and muzzle (1/2 point) dermatitis (3).

Proteinuria was screened using Albustix (Siemens). Plasma was obtained by cardiac puncture. Kidneys were removed, bisected, formalin-fixed, paraffin embedded, and H&E stained. Kidneys were scored for glomerulonephritis on a scale of 1-6 and interstitial nephritis on a scale of 1-4 in a blinded manner by M.K. (F2 cohort) or S.B. (backcrossed cohort) (2).

Flow Cytometry

Flow cytometry was performed as previously described (2). In brief, spleens and bone marrow were homogenized and red blood cells were lysed using Ammonium-Chloride-Potassium buffer (prepared in-house). Cells were resuspended in Phosphate Buffered Saline (PBS) with 3% calf serum and the FcR-blocking antibody 2.4G2. Live/dead discrimination was performed using fixable viability stain 510 (BD) or ethidium monoazide bromide (Invitrogen). Surface and intracellular staining antibodies are listed below. Cells were fixed in 1% paraformaldehyde or

Cytofix/Cytoperm (BD) where appropriate. Data were obtained using a LSRII (BD) with FACS DIVA software and analyzed using FlowJo.

Antibodies used for FACS staining

Antibodies used for FACS surface and intracellular staining were as follows: IA/E-PE (Biolegend, M5/114.15.2), Bst-2-biotin (in-house conjugated, 927), CD11c-PE/Cy7 (BD Pharmigen, HL3), CD45R-APC/Cy7 (BD Pharmigen, RA3-6B2), SiglecH-Al647 (eBioscience, eBio440c), CD19-Pacblue (in-house conjugated, 1D3.2), Ly6G-Al488 (in-house conjugated, 1A8), Gr1-PE/Cy7 (Biolegend, RB6-8C5), Gr1-PE (Biolegend, RB6-8C5), CD11b-APC/Cy7 (Biolegend, M1/70), CD11b-PE (Biolegend, M1/70), F4/80-Al647 (in-house conjugated, BM8), F4/80-APC (Biolegend, BM8), CD44-Al488 (in-house conjugated, 1M7), CD44-APC-Cy7 (Biolegend, 1M7), TcRβ-APC/Cy7 (Biolegend, H57-597), TCRβ-PE/Cy7, (Biolegend, H57-597), CD62L-PE/Cy7 (Biolegend, Mel-14), CD8-Al647 (in-house conjugated, TIB 105), CD4-PE (Biolegend, GK1.5), CD138-PE (BD Pharmigen, 281-2), CD19-AI647 (in-house conjugated, 1D3.2), kappa-AI488 (in-house conjugated, 187.1), and Ly6B.2-Fitc (AbD Serotec, 7/4).

ELISpot assays

AFC producing κ light chain antibodies, IgG1, IgG2a, or IgM were detected by ELISpot as previously described (4). In brief, 96-well Immulon 4 HBX plates were coated overnight at 4°C with 5 mg/ml polyclonal goat-anti mouse κ (Southern Biotech; 1050-01). Nonspecific binding was blocked with 1% bovine serum albumin in PBS and samples were incubated at 37°C. Alkaline phosphatase-conjugated secondary antibodies (Southern Biotech; Igκ [1050-04], IgG1 [1070-04],

IgG2a [1080-04], or IgM [1020-04]) were detected with bromo-4-chloro-3-indolyl phosphate substrate (Southern Biotech).

ELISAs

Anti-Sm, anti-nucleosome, anti-RNA, rheumatoid factor, total IgM, and IgG ELISAs were performed as previously described (2, 5-8). Specific antibodies were detected with alkaline phosphatase-conjugated goat anti-mouse IgG (Southern Biotech [1030-04]). The monoclonal antibodies Y2, BWR4, 400tμ23, PL4-2 or PL2-3 (in-house) were used as standards for the anti-Sm, anti-RNA, rheumatoid factor, and anti-nucleosome measurements respectively.

Reverse Passive Arthus reaction in the cremaster muscle

The RPA reaction in the cremaster muscle was performed as described previously (9). Briefly, anti-BSA antibody (200 μg/300 μL, Sigma Aldrich) was injected parascrotally, followed by the intravenous injection of BSA (300 μg/100 μL, Sigma Aldrich). Leukocyte recruitment and NET formation was evaluated 3 hours later. NET formation was visualized by injection of 25 mmol Sytox Green (9), and the number of Sytox Green positive NET-like structures were counted in 6-9 fields per view. Leukocyte adhesion and transmigration were evaluated as described previously (10). In experiments using Cl-Amidine (Millipore), mice received 10 mg/kg of Cl-Amidine or vehicle control (DMSO in PBS) via i.p. injection either 1h before the experiment or for 3 consecutive days with the last dose 20h before the experiment (11).

Serum transfer SLE nephritis

To induce nephritis using serum transfer (12), mice transgenically expressing the FcγRIIA and additionally lacking the Fc γ-chain and Mac-1 (IIA$\gamma^{-/-}$Mac-1$^{-/-}$) were injected s.c. in both flanks with 2.5 µg of human IgG (Jackson ImmunoResearch Laboratories) in complete Freund's adjuvant (Thermo Scientific) on day -3. On days 0 and 2, 200µl of sterile serum was injected i.v. Spot urine was collected on day 0, 7, 10, and day 14 after injection. Kidneys were collected at day 10 or day 14 for histological and FACS analysis as described previously (13). Albumin in the urine was evaluated by ELISA (Bethyl laboratory) and creatinine was measured using a chemical test (Cayman Chemicals) as previously reported (12). Mice received either vehicle control (PBS) or Cl-Amidine at 10 mg/kg/d (11) in 200µl i.p. for the duration of the experiment.

Anti-GBM Nephritis

Experimental anti-GBM nephritis was induced as previously reported (14). Briefly, mice expressing the FcγRIIA but lacking the Fc γ-chain (IIA$\gamma^{-/-}$) were preimmunized in the right footpad with 0.05 mg of rabbit IgG (Jackson ImmunoResearch Laboratories) in Freund incomplete adjuvant (Thermo Fisher) and non-viable desiccated mycobacterium tuberculosis H37Ra (Difco). The mice were injected intravenously with 25µl of heat-inactivated, filter-sterilized rabbit nephrotoxic serum. The kidneys were harvested at day 7 and 14. Spot urine samples were collected at indicated time points after serum injection. Mice received either vehicle control (PBS) or Cl-Amidine at 10 mg/kg/d (11) in 200µl i.p. for the duration of the experiment.

References

1. Nickerson KM, Cullen JL, Kashgarian M, and Shlomchik MJ. Exacerbated autoimmunity in the absence of TLR9 in MRL.Fas(lpr) mice depends on Ifnar1. *J Immunol.* 2013;190(8):3889-94.
2. Campbell AM, Kashgarian M, and Shlomchik MJ. NADPH oxidase inhibits the pathogenesis of systemic lupus erythematosus. *Sci Transl Med.* 2012;4(157):157ra41.
3. Berland R, Fernandez L, Kari E, Han JH, Lomakin I, Akira S, et al. Toll-like receptor 7-dependent loss of B cell tolerance in pathogenic autoantibody knockin mice. *Immunity.* 2006;25(3):429-40.
4. Teichmann LL, Schenten D, Medzhitov R, Kashgarian M, and Shlomchik MJ. Signals via the adaptor MyD88 in B cells and DCs make distinct and synergistic contributions to immune activation and tissue damage in lupus. *Immunity.* 2013;38(3):528-40.
5. Nickerson KM, Christensen SR, Shupe J, Kashgarian M, Kim D, Elkon K, et al. TLR9 regulates TLR7- and MyD88-dependent autoantibody production and disease in a murine model of lupus. *J Immunol.* 2010;184(4):1840-8.
6. Christensen SR, Kashgarian M, Alexopoulou L, Flavell RA, Akira S, and Shlomchik MJ. Toll-like receptor 9 controls anti-DNA autoantibody production in murine lupus. *J Exp Med.* 2005;202(2):321-31.
7. Monestier M, and Novick KE. Specificities and genetic characteristics of nucleosome-reactive antibodies from autoimmune mice. *Mol Immunol.* 1996;33(1):89-99.

8. Blanco F, Kalsi J, and Isenberg DA. Analysis of antibodies to RNA in patients with systemic lupus erythematosus and other autoimmune rheumatic diseases. *Clin Exp Immunol.* 1991;86(1):66-70.

9. Chen K, Nishi H, Travers R, Tsuboi N, Martinod K, Wagner DD, et al. Endocytosis of soluble immune complexes leads to their clearance by FcgammaRIIIB but induces neutrophil extracellular traps via FcgammaRIIA in vivo. *Blood.* 2012;120(22):4421-31.

10. Herter JM, Rossaint J, Block H, Welch H, and Zarbock A. Integrin activation by P-Rex1 is required for selectin-mediated slow leukocyte rolling and intravascular crawling. *Blood.* 2013;121(12):2301-10.

11. Knight JS, Zhao W, Luo W, Subramanian V, O'Dell AA, Yalavarthi S, et al. Peptidylarginine deiminase inhibition is immunomodulatory and vasculoprotective in murine lupus. *J Clin Invest.* 2013;123(7):2981-93.

12. Rosetti F, Tsuboi N, Chen K, Nishi H, Ernandez T, Sethi S, et al. Human lupus serum induces neutrophil-mediated organ damage in mice that is enabled by Mac-1 deficiency. *J Immunol.* 2012;189(7):3714-23.

13. Herter JM, Rossaint J, Spieker T, and Zarbock A. Adhesion molecules involved in neutrophil recruitment during sepsis-induced acute kidney injury. *J Innate Immun.* 2014;6(5):597-606.

14. Tsuboi N, Asano K, Lauterbach M, and Mayadas TN. Human neutrophil Fcgamma receptors initiate and play specialized nonredundant roles in antibody-mediated inflammatory diseases. *Immunity.* 2008;28(6):833-46.

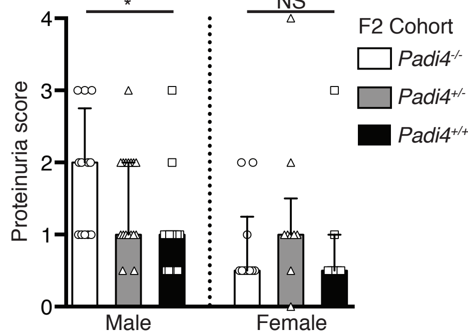

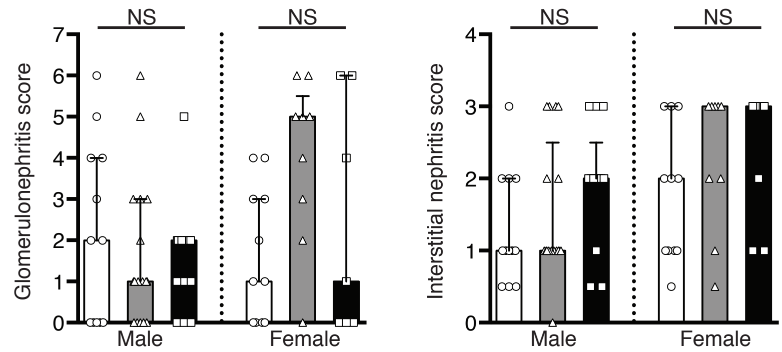

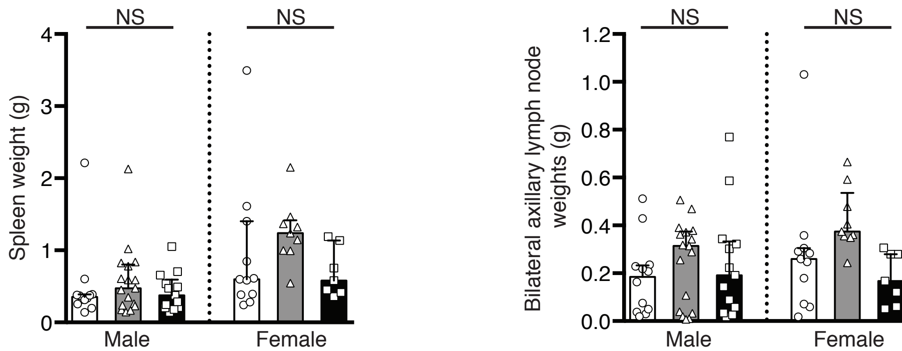

Supplemental Figure 1. Padi4 deficiency results in increased proteinuria in male mice but does not otherwise impact lupus nephritis or lymphadenopathy/splenomegaly in the F2 cohort. (A) Proteinuria score (*Padi4*$^{-/-}$ males n=12; *Padi4*$^{-/+}$ males n=17; *Padi4*$^{+/+}$ males n=13; *Padi4*$^{-/-}$ females n=10; *Padi4*$^{-/+}$ females n=9; *Padi4*$^{+/+}$ females n=7). **(B)** Glomerulonephritis (left panel) and interstitial nephritis (right panel) scores. **(C)** Spleen (left panel) and axillary lymph node (right panel) weights. Scores and weights are represented as a function of *Padi4* genotype and gender at 16 weeks of age. Bars represent the median ± interquartile range. A Kruskal-Wallis test with post-hoc Dunn's test was performed to determine statistical significance within each gender (*Padi4*$^{-/-}$ males n=12; *Padi4*$^{-/+}$ males n=17; *Padi4*$^{+/+}$ males n=13; *Padi4*$^{-/-}$ females n=11; *Padi4*$^{-/+}$ females n=9; *Padi4*$^{+/+}$ females n=7 unless otherwise indicated). NS, not significant.

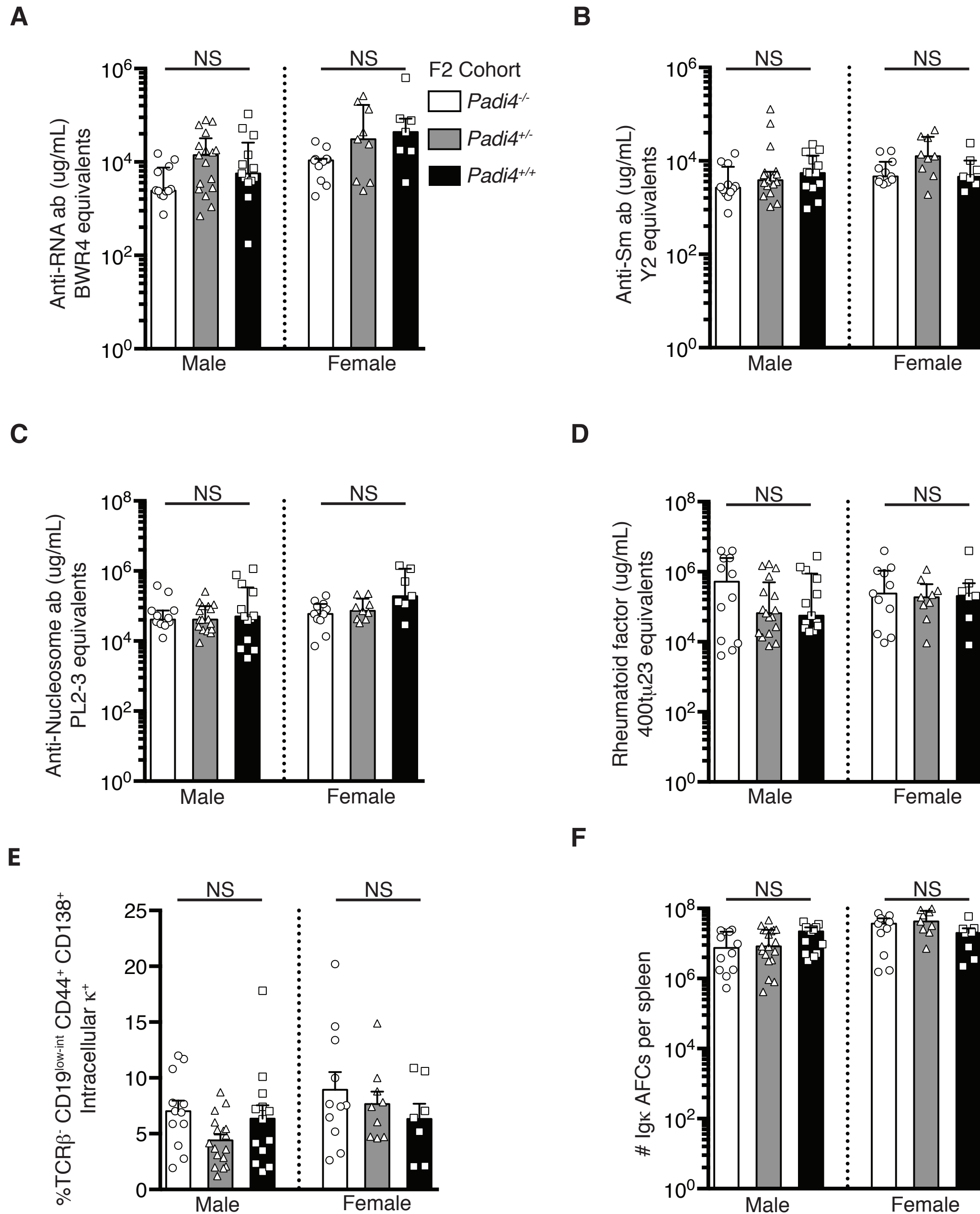

Supplemental Figure 2. Padi4 deficiency does not significantly alter the anti-self-response or the AFC compartment in F2 mice. (A-D) Serum anti-RNA (A), anti-SM (B), anti-nucleosome (C), and rheumatoid factor (D) titers at 16 weeks of age. **(E)** Percentage of TCRβ$^-$ CD44$^+$ CD138$^+$ intracellular κ$^+$ antibody forming cells (AFCs) in spleens. (**F**) Numbers of Igκ$^+$ AFCs per spleen were determined by ELISpot (*Padi4*$^{-/-}$ males n=12; *Padi4*$^{-/+}$ males n=19; *Padi4*$^{+/+}$ males n=13; *Padi4*$^{-/-}$ females n=11; *Padi4*$^{-/+}$ females n=9; *Padi4*$^{+/+}$ females n=8). For panels A-D and F data representation, statistics and number of mice are as in supplemental figure 1 unless otherwise indicated. In panel E bar graphs are represented as the mean ± SEM and a one-way ANOVA with post-hoc Holm-Sidak test was performed to determine statistical significance within each gender. NS, not significant.

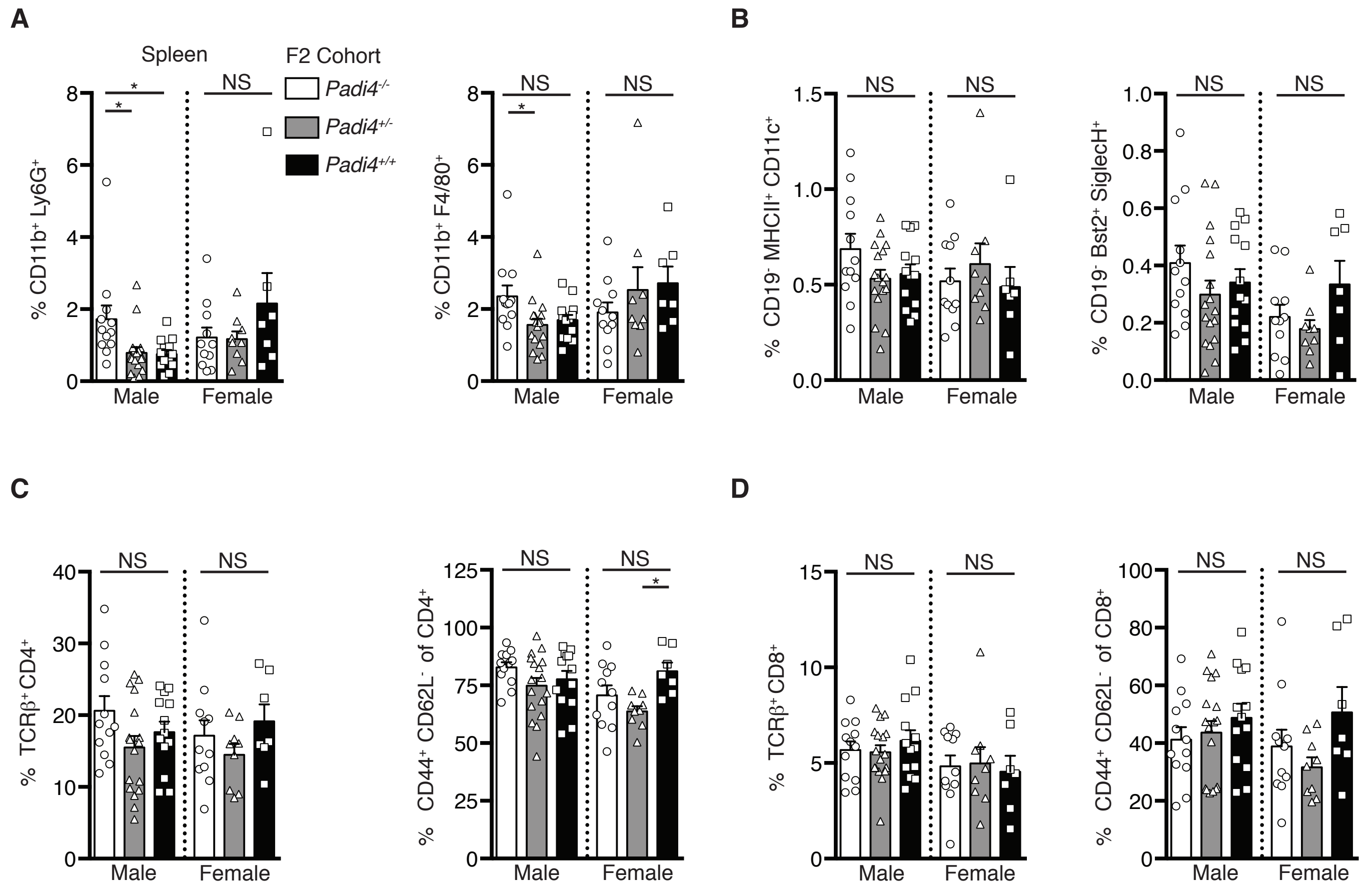

Supplemental Figure 3. ***Padi4*** **genotype increased the percentage of macrophages and neutrophils in male mice but does not otherwise affect the myeloid, DC, or T cell compartments in the F2 cohort.** **(A)** Percentage of live $CD11b^+$ $Ly6G^+$ neutrophils and $CD11b^+$ $GR1^{lo\text{-}int}$ $F4/80^+$ macrophages in the spleens. **(B)** Percentage of live $CD19^-$ $MHCII^+$ $CD11c^+$ conventional dendritic cells (DCs) (left panel) and $CD19^-$ $BST2^+$ $CD11c^+$ plasmacytoid DCs (right panel). **(C)** Percentage of live $TCR\beta^+$ $CD4^+$ T cells (left panel) and of $CD4^+$ $CD44^+$ $CD62L^-$ activated T cells (right panel). **(D)** Percentage of live $TCR\beta^+$ $CD8^+$ T cells (left panel) and of $CD8^+$ $CD44^+$ $CD62L^-$ activated T cells (right panel). Mice were analyzed at 16 weeks of age. Bar graphs are represented as the mean ± SEM and a one-way ANOVA with post-hoc Holm-Sidak test was performed to determine statistical significance within each gender (*Padi4*$^{-/-}$ males n=12; *Padi4*$^{-/+}$ males n=17; *Padi4*$^{+/+}$ males n=13; *Padi4*$^{-/-}$ females n=11; *Padi4*$^{-/+}$ females n=9; *Padi4*$^{+/+}$ females n=7). * indicates P<0.05, NS, not significant